

## XRD and impedance spectroscopy study of phase transitions in nanocrystalline Li–Mn spinels

*D.V.Lisovytskiy, V.N.Baumer\**

Institute of Physical Chemistry, Polish Academy of Sciences,  
Kasprzaka 44/52, 01-224 Warszawa, Poland

\*STC "Institute for Single Crystals", National Academy of Sciences of  
Ukraine, 60 Lenin Ave, 61001 Kharkiv, Ukraine

*Received October 7, 2007*

Phase transition in nanocrystalline lithium manganese spinels synthesized by sol-gel technique in laboratory and in commercially available  $\text{LiMn}_2\text{O}_4$  powders was studied. In addition to the standard impedance measurements and the X-ray diffraction in Bragg-Brentano geometry, simultaneous measurements of impedance spectrum and X-ray pattern in non-focusing geometry were performed in the temperature range between  $-25$  and  $+100^\circ\text{C}$ . Using Rietveld refinement, the phase composition of samples has been estimated quantitatively.

Исследованы фазовые переходы в нанокристаллических Li–Mn шпинелях, синтезированных методом золь-гель в лабораторных условиях, и в коммерческих порошках  $\text{LiMn}_2\text{O}_4$ . Кроме стандартных измерений методами импедансной спектроскопии и рентгеновским при геометрии Брегга-Брентано, проведены одновременные измерения методами импедансной спектроскопии и рентгеновским при нефокусирующей геометрии в температурном диапазоне от  $-25^\circ\text{C}$  до  $+100^\circ\text{C}$ . С использованием ритвельдовского анализа количественно оценен фазовый состав образцов.

Lithium manganese spinels are one of the most promising materials for the electrodes of modern Li-ion rechargeable batteries because of their low cost and low toxicity in comparison with the compounds now in use. Taking into account the considerable interest in nanocrystalline systems which in many instances exhibit unusual properties as compared to the bulk materials, it is that batteries constructed on the base of nanocrystalline spinel electrodes are generally anticipated to have much better properties and usable as energy sources not only for portable electronic devices but also for electric vehicles. However, the conductivity of  $\text{LiMn}_2\text{O}_4$  can be affected by phase transformation between cubic (Fd-3m) and orthorhombic (Fddd) structure which occurs

near room temperature. The structure transformation is visible in the X-ray pattern as splitting of sensitive reflections. On cooling, the 400 reflection of the cubic phase splits in the orthorhombic phase into 400, 040, and 004 ones. This phase transformation is accompanied by a considerable decrease of conductivity.

Of special interest in material studies are simultaneous measurements of different parameters. For the all investigated samples in addition to standard XRD in Bragg-Brentano geometry measurements, simultaneous measurements of impedance spectra and X-ray pattern in non-focusing geometry were performed in the temperature range from  $-25^\circ\text{C}$  to  $+100^\circ\text{C}$ . For this purpose, specific equipment was constructed and used. In

this way, a correlation between the XRD profile parameters and electrical properties calculated from impedance spectra was evidenced.

The experimental setup had to fulfill the following requirements: a) to provide fast XRD data collection in reflection geometry; b) to provide impedance measurements on the sample simultaneously with XRD data collection (or at predetermined sequence); c) to allow measurements under controlled atmosphere at a programmed sequence of stabilized temperatures both below and above room temperature.

The developed experimental setup for simultaneous impedance and X-ray measurements combines AutoLab PGSTAT 30 Frequency Response Analyzer with Siemens D5000 diffractometer. The impedance was measured in the frequency range from 10 MHz to 0.1 Hz, at the signal rms amplitude of 20 mV. The diffractometer was equipped with graphite monochromator in the incident beam and an INEL CPS-120 curved position sensitive detector. The measurements on manganese spinel samples were performed in the temperature range from  $-25^{\circ}\text{C}$  to  $+100^{\circ}\text{C}$  using a special camera described in [1] placed in the goniometer center. The sample, in a mechanically stable form (a pellet) with thin metal films sputtered on opposite faces, is placed on copper plate in thermal contact with Peltier element. A K-type shielded thermocouple is used as temperature sensor in combination with a Eurotherm 2416 controller. The cell can be flushed with dry air or helium in order to avoid water vapor condensation or ice deposition on the sample surface at temperatures below  $0^{\circ}\text{C}$ . The measurement program allows multiple heating and cooling temperature ramps and temperature stabilization within preset criteria. Independently, the X-ray diffraction measurements were also made in Bragg-Brentano geometry.

In this work, three kinds of samples were investigated: (i) stoichiometric spinel  $\text{LiMn}_2\text{O}_4$  (SH) and  $\delta$ -spinel  $\text{Li}_{1.005}\text{Mn}_{1.995}\text{O}_4$  (DH) prepared from powders synthesized by sol-gel technique as described in [2, 3] and heat treated at  $800^{\circ}\text{C}$ , this group of samples being obtained from authors of [2]; (ii) prepared from commercially available powders of  $\text{LiMn}_2\text{O}_4$ : supplied by Alfa Aesar and Sigma-Aldrich (Alfa and Aldrich, respectively); (iii) prepared from the same commercial powders by heat treatment at  $800^{\circ}\text{C}$  for 24 h followed by rapid cooling (Alfa800 and Aldrich800, respectively). For imped-

ance measurements, copper electrodes were sputtered on the polished faces of sintered pellets.

Stoichiometric  $\text{LiMn}_2\text{O}_4$  and slightly Li substituted  $\text{Li}_{1.005}\text{Mn}_{1.995}\text{O}_4$  spinels obtained by sol-gel method and heat-treated at  $800^{\circ}\text{C}$  exhibited phase transition from cubic to orthorhombic structure upon cooling below room temperature. The transition was evidenced by splitting of the 400 X-ray reflection and by anomalies in the temperature dependence of conductivity. In the case of stoichiometric  $\text{LiMn}_2\text{O}_4$ , the conductivity decreased by a factor of about 10 during measurements. During the phase transformation, the conductivity changes were well correlated with changes in the X-ray diffraction pattern shape near the 400 reflection. There is clear distinction between the single 400 peak observed at temperatures above  $20^{\circ}\text{C}$  and the broad intensity maximum seen at low temperatures. During further cooling down to  $-25^{\circ}\text{C}$  and subsequent heating, virtually no changes of the X-ray diffraction pattern were recorded up to  $20^{\circ}\text{C}$ . Above this temperature, a reverse transition from orthorhombic to cubic structure took place. A narrow peak, characteristic for cubic phase, appeared at  $40^{\circ}\text{C}$  and remained unchanged on heating to  $100^{\circ}\text{C}$  and subsequent cooling to  $17^{\circ}\text{C}$ . A similar behavior was observed for  $\text{Li}_{1.005}\text{Mn}_{1.995}\text{O}_4$  sample (Fig. 1a). In Fig. 2, together with the resistivity of the stoichiometric spinel and Li substituted spinel, the FWHM of the 400 reflection is also plotted as a function of temperature. It is seen that the thermal hysteresis of the FWHM was well correlated with that of resistivity. In stoichiometric  $\text{LiMn}_2\text{O}_4$ , the thermal hysteresis of the resistivity and of the 400 reflection FWHM extends over a wider temperature range than in the lithium substituted spinel  $\text{Li}_{1.005}\text{Mn}_{1.995}\text{O}_4$ .

The sample prepared from powder supplied by Alfa Aesar and heat-treated at  $800^{\circ}\text{C}$ , similarly to the samples synthesized by sol-gel technique, exhibited phase transition from cubic to orthorhombic structure upon cooling below room temperature. The structural transition, clearly visible in the X-ray pattern as the 400 reflection splitting, was accompanied by an increase in resistivity by a factor of about 10. The thermal hysteresis of resistivity was well correlated with that of the 400 reflection FWHM (Fig. 2c), however, it extended over a narrower temperature range than for the samples prepared by the sol-gel method.

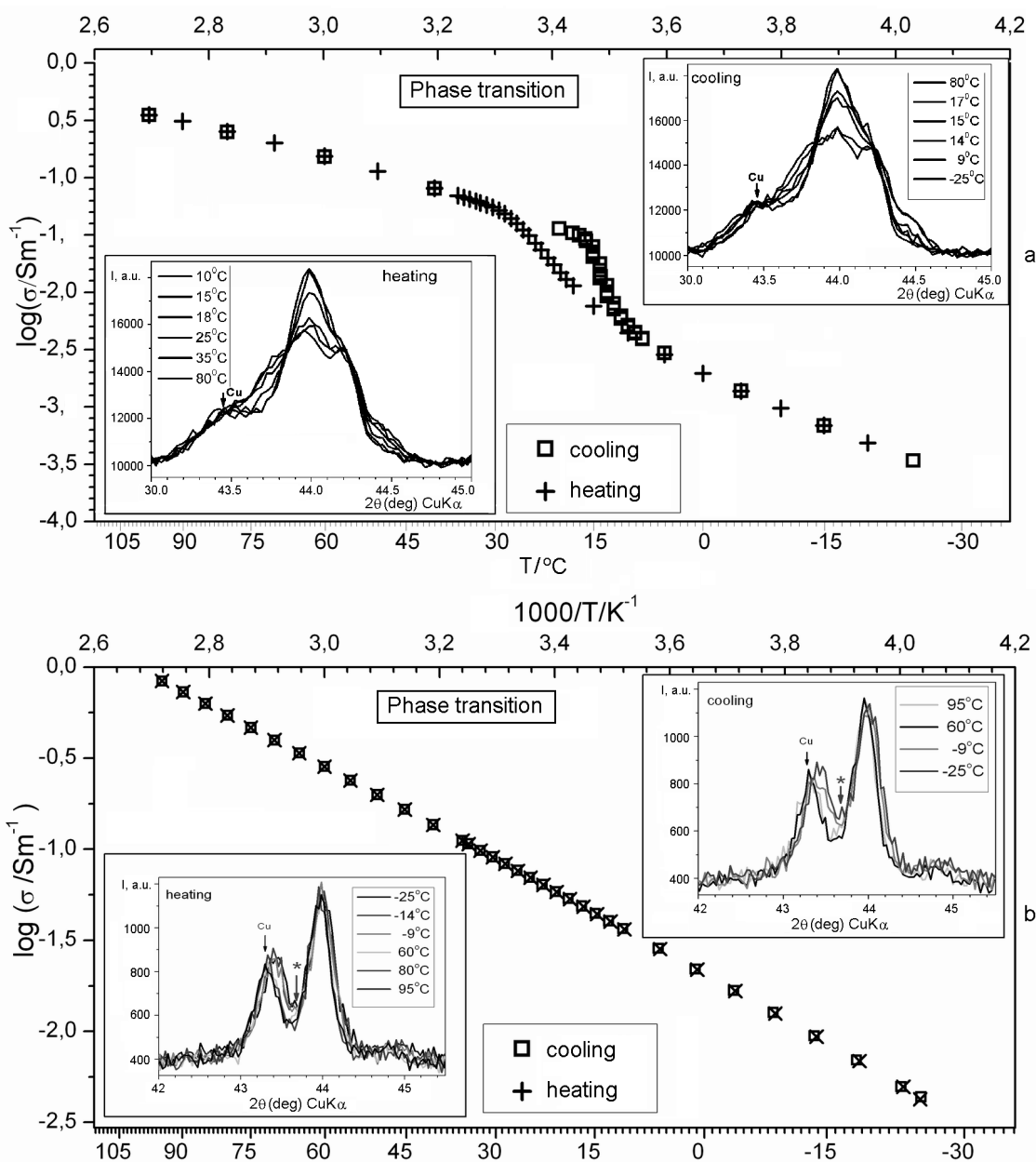


Fig. 1. Temperature dependences of conductivity correlated with 400 peak shape: a) for  $\text{Li}_{1.005}\text{Mn}_{1.995}\text{O}_4$  obtained by sol-gel method (DH), b) for  $\text{LiMn}_2\text{O}_4$  sample obtained from Sigma-Aldrich Co. and heat-treated at  $800^\circ\text{C}$  (Aldrich800).

In the case of sample prepared from powder supplied by Sigma-Aldrich and heat-treated at  $800^\circ\text{C}$ , there was no stepwise change of resistivity observed upon cooling or heating in the temperature range between  $100^\circ\text{C}$  and  $-25^\circ\text{C}$  (Fig. 2d). The 400 reflection FWHM increased only slightly upon cooling from  $100^\circ\text{C}$  to  $-25^\circ\text{C}$ . There was no signs of thermal hysteresis neither for resistivity nor for FWHM. Although the phase transition was not detected in the conductivity measurements, the X-ray pattern measured with the position sensitive

detector indicated pure cubic phase above room temperature, while at low temperatures, there was some broadening of the 400 reflection and an increased intensity around  $43.7^\circ(2\theta)$ , between the 400 maximum and the 111 reflection from the Cu film serving as electrode. The Rietveld analysis of the X-ray diffraction pattern measured in the Bragg-Brentano geometry at  $-25^\circ\text{C}$  indicated a mixture of two coexistent phases: cubic and orthorhombic. Thus, the phase transition from cubic to orthorhombic structure was in progress but not complete

Table. Numerical results of Rietveld refinement for all investigated samples

| Sample,<br>$T_{meas}$ (°C) | Cell parameters of the<br>individual phases [Å]   | Wt.<br>Fract.(%)                  | Vol. [Å <sup>3</sup> ]     | Bragg R-fact.         | RF factor            |
|----------------------------|---|-----------------------------------|----------------------------|-----------------------|----------------------|
| SH, 25                     | LiMn <sub>2</sub> O <sub>4</sub> <b>Cubic</b><br>$a = 8.2475(2)$  | 100                               | 561.0                      | 2.89                  | 2.31                 |
| DH, 25                     | Li <sub>1.005</sub> Mn <sub>1.995</sub> <b>Cubic</b><br>$a = 8.2448(5)$   | 100                               | 560.45                     | 3.75                  | 2.81                 |
| SH-4                       | LiMn <sub>2</sub> O <sub>4</sub> , <b>Orthorhombic</b> ,<br>$a = 8.2075(2)$ , $b = 8.2537(2)$ ,<br>$c = 8.2860(2)$  | 100                               | 561.31                     | 5.08                  | 3.84                 |
| DH-4                       | Li <sub>1.005</sub> Mn <sub>1.995</sub> <b>Orthorhombic</b><br>$a = 8.2084(3)$ , $b = 8.2505(3)$ ,<br>$c = 8.2849(3)$   | 100                               | 561.08                     | 5.31                  | 4.34                 |
| Alfa 50                    | 1) LiMn <sub>2</sub> O <sub>4</sub> <b>Cubic</b> $a = 8.2408(6)$<br>2) Mn <sub>3</sub> O <sub>4</sub> <b>Tetragonal</b><br>$a = 5.7651(8)$ , $c = 9.4422(8)$  | 97(1)<br>3.13(22)                 | 559.63<br>313.82           | 15.4<br>35.2          | 8.90<br>31.3         |
| Alfa<br>-25                | 1) LiMn <sub>2</sub> O <sub>4</sub> <b>Orthorhombic</b><br>$a = 8.2052(9)$ , $b = 8.2417(9)$ ,<br>$c = 8.2778(9)$<br>2) Mn <sub>3</sub> O <sub>4</sub> <b>Tetragonal</b><br>$a = 5.7651(8)$ , $c = 9.4422(8)$   | 97(1)<br>3.13(22)                 | 559.78<br>313.82           | 13.6<br>45.5          | 10.4<br>35.8         |
| Alfa 800<br>50             | 1) LiMn <sub>2</sub> O <sub>4</sub> <b>Cubic</b> $a = 8.2539(6)$<br>2) Mn <sub>3</sub> O <sub>4</sub> <b>Tetragonal</b><br>$a = 5.7651(8)$ , $c = 9.4422(8)$  | 98.99(60)<br>1.01(5)              | 562.31<br>313.82           | 9.05<br>60.6          | 7.94<br>42.1         |
| Alfa 800<br>-25            | 1) LiMn <sub>2</sub> O <sub>4</sub> <b>Orthorhombic</b><br>$a = 8.2052(9)$ , $b = 8.2554(9)$ ,<br>$c = 8.2906(9)$<br>2) Mn <sub>3</sub> O <sub>4</sub> <b>Tetragonal</b> $a =$<br>$5.7651(8)$ , $c = 9.4422(8)$   | 98.99(61)<br>1.01(5)              | 561.58<br>313.82           | 9.62<br>77.6          | 8.94<br>51.4         |
| Aldrich<br>50              | 1) LiMn <sub>2</sub> O <sub>4</sub> <b>Cubic</b> $a = 8.2433(7)$<br>2) Li <sub>2</sub> MnO <sub>3</sub> <b>Monoclinic</b><br>$a = 4.9246(6)$ , $b = 8.5216(6)$ ,<br>$c = 5.0245(6)$ , $\beta = 109.398(3)^\circ$  | 95.06(28)<br>4.94(1)              | 560.14<br>198.89           | 7.57<br>56.9          | 7.52<br>49.1         |
| Aldrich<br>-25             | 1) LiMn <sub>2</sub> O <sub>4</sub> <b>Orthorhombic</b><br>$a = 8.2063(5)$ , $b = 8.2423(5)$ ,<br>$c = 8.2907(5)$<br>2) LiMn <sub>2</sub> O <sub>4</sub> <b>Cubic</b> $a = 8.2379(7)$<br>3) Li <sub>2</sub> MnO <sub>3</sub> <b>Monoclinic</b><br>$a = 4.9246(6)$ , $b = 8.5216(6)$ ,<br>$c = 5.0245(6)$ , $\beta = 109.398(3)^\circ$ | 62.64(21)<br>32.42(8)<br>4.94(1)  | 560.77<br>559.04<br>198.89 | 11.5<br>8.09<br>55.5  | 8.45<br>7.82<br>38.4 |
| Aldrich 800<br>50          | 1) LiMn <sub>2</sub> O <sub>4</sub> <b>Cubic</b><br>$a = 8.2446(5)$<br>2) Li <sub>2</sub> MnO <sub>3</sub> <b>Monoclinic</b><br>$a = 4.9246(6)$ , $b = 8.5216(6)$ ,<br>$c = 5.0245(6)$ , $\beta = 109.398(3)^\circ$   | 96.55(60)<br>3.45(7)              | 560.41<br>198.89           | 8.55<br>65.7          | 7.07<br>44.0         |
| Aldrich 800<br>-25         | 1) LiMn <sub>2</sub> O <sub>4</sub> <b>Orthorhombic</b><br>$a = 8.2065(5)$ , $b = 8.2409(5)$ ,<br>$c = 8.2902(5)$<br>2) LiMn <sub>2</sub> O <sub>4</sub> <b>Cubic</b> $a = 8.2451(7)$<br>3) Li <sub>2</sub> MnO <sub>3</sub> <b>Monoclinic</b><br>$a = 4.9246(6)$ , $b = 8.5216(6)$ ,<br>$c = 5.0245(6)$ , $\beta = 109.398(3)^\circ$ | 49.64(73)<br>46.80(65)<br>3.56(6) | 560.65<br>560.51<br>198.89 | 13.1<br>10.21<br>58.4 | 12.4<br>7.42<br>47.6 |

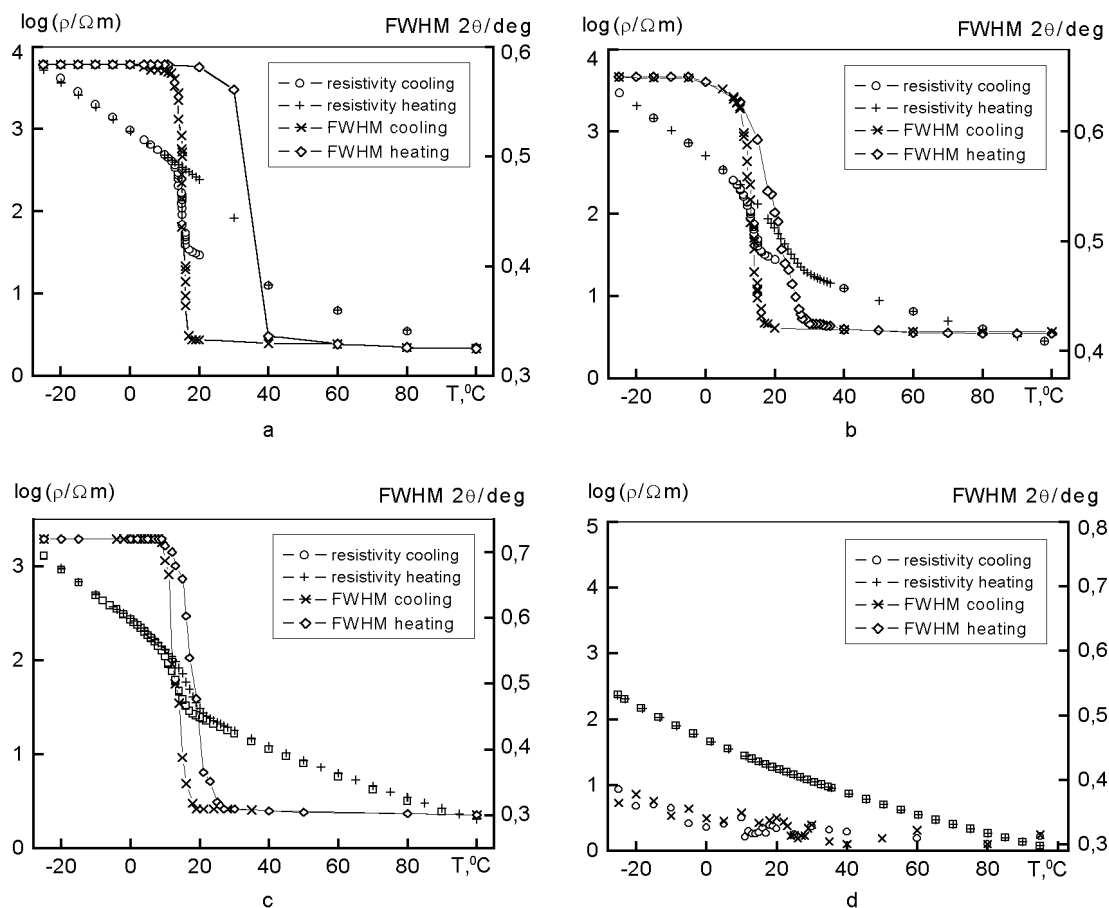


Fig. 2. Temperature dependences of the 400 reflection or triplet: 400, 040, 004 (fitted as one peak) FWHM measured simultaneously with resistivity for a)  $\text{LiMn}_2\text{O}_4$  obtained by sol-gel method (SH); b)  $\text{Li}_{1.005}\text{Mn}_{1.995}\text{O}_4$  obtained by sol-gel method (DH); c)  $\text{LiMn}_2\text{O}_4$  obtained from Alfa Aesar Co. and heat-treated at  $800^\circ\text{C}$  (Alfa800), d)  $\text{LiMn}_2\text{O}_4$  obtained from Sigma-Aldrich Co. and heat-treated at  $800^\circ\text{C}$  (Aldrich 800).

even after cooling to  $-25^\circ\text{C}$ . The Rietveld refinement results for the X-ray patterns of the studied samples are summarized in Table. The phase analysis based on the Rietveld refinement proved that the samples prepared from powders obtained by sol-gel method and heat treated at  $800^\circ\text{C}$  are single phase (cubic above room temperature, orthorhombic below  $0^\circ\text{C}$ ). The cubic phase lattice constant of the lithium substituted spinel  $\text{Li}_{1.005}\text{Mn}_{1.995}\text{O}_4$  is slightly smaller than that of the stoichiometric spinel  $\text{LiMn}_2\text{O}_4$ , in agreement with the dependence of the lattice constant on composition for the series of solid solutions  $\text{Li}_{1+x}\text{Mn}_{2-x}\text{O}_4$  [4, 5].

According to the phase analysis by Rietveld refinement, the powder supplied by Alfa Aesar contained  $\text{Mn}_3\text{O}_4$  as an impurity phase, the content thereof being decreased from 3 % to 1 % in the course of annealing at  $800^\circ\text{C}$ . After annealing, the lattice constant of the cubic spinel phase is larger

than in as-received powder, which indicates that the molar ratio of manganese to lithium increased due to incorporation of manganese from the impurity oxide  $\text{Mn}_3\text{O}_4$ . The powder supplied by Sigma-Aldrich contained  $\text{Li}_2\text{MnO}_3$  as an impurity phase, the content thereof was about 5 % and decreased to 3.5 % upon heat treatment at  $800^\circ\text{C}$ . The lattice constant of the cubic spinel, which is the major phase above room temperature, did not change significantly as a result of annealing, thus, no changes of the spinel phase composition can be evidenced. The phase analysis of the X-ray diffraction patterns measured at  $-25^\circ\text{C}$  for the powder supplied by Sigma-Aldrich showed coexistence of the orthorhombic and cubic phases. The calculated weight fraction of the two phases indicated that the content of the cubic phase at  $-25^\circ\text{C}$  remained higher in the powder annealed at  $800^\circ\text{C}$  than in the as-received powder. However, it is worth noting

that the results of phase analysis by means of the Rietveld profile refinement should be treated with caution, since the anisotropy of additional phases can cause overestimation of their fraction in the system, as demonstrated by Massarotti et al. for an analogous case of the coexistent phases:  $\text{LiMn}_2\text{O}_4$  and  $\text{Li}_2\text{MnO}_3$  [6]. Furthermore, the weight fractions of the cubic and orthorhombic spinel phases, obtained by Rietveld refinement of the XRD profiles measured at  $-25^\circ\text{C}$  for powder supplied by Sigma-Aldrich, seem to indicate evolution of phase content resulting from annealing, which is in disagreement with the results of impedance measurements. As is seen in Fig. 1b, the measured conductivity showed a deviation from the Arrhenius type linear dependence of the logarithm of conductivity on the inverse temperature in the case of the Sigma-Aldrich sample sintered at  $800^\circ\text{C}$ , whereas presence such deviation is not observed for the sample prepared from the as-received powder. As a matter of fact, the conductivity of samples, which are pressed from the as-received powder, above room temperature is roughly an order of magnitude lower than conductivity of samples sintered at  $800^\circ\text{C}$ , for samples supplied by Alfa Aesar as well as by Sigma-Aldrich. The difference in conductivity is likely to be due to poor contact between crystallites in pressed samples, which becomes vastly improved by sintering, thus removing constrictions to current flow.

The average crystallite sizes, as estimated from the full width at half maximum of the cubic spinel 222 reflection, are very similar for all studied samples, and amount about 40 nm. The average crystallite size calculated from the width of X-ray diffraction peak should be more precisely interpreted as the size of coherent diffraction areas in polycrystalline material and should not be confused with grain size. The present findings that the coherent scattering areas are of similar size in the four studied samples heat-treated at  $800^\circ\text{C}$  irrespectively of the  $\text{LiMn}_2\text{O}_4$  powder origin indicate that the crystal structure of lithium manganese oxide spinel does not conform to perfect translational symmetry. Both the cubic phase and the orthorhombic phase appear to exhibit a mosaic domain structure of nanometer size. The imperfect crystal structure may be a result of the structural phase transition from cubic to orthorhombic symmetry.

The magnitude of conductivity change accompanying the phase transition from cubic to orthorhombic structure seems to depend on the presence of impurity phases. The decrease of  $\text{Li}_2\text{MnO}_3$  fraction in the Sigma-Aldrich sample caused by heat treatment at  $800^\circ\text{C}$  coincided with conductivity decrease during the phase transition, which was not observed for the sample pressed from as-received powder. A distinctive increase of the conductivity anomaly was observed for Alfa-Aesar sample in which the fraction of the additional phase  $\text{Mn}_3\text{O}_4$  was reduced by heat treatment. A plausible explanation for these phenomena is a change in the actual stoichiometry of the spinel phase, which is known to influence the course of phase transition [7–11]. The presence of additional phases may also disturb the local environment, introducing charge disorder into orthorhombic structure and preserving easy conductivity pathways. The conductivity is also influenced by evolution of the microstructure during sintering which improves the intergranular contact. The variations in the pattern of temperature dependence of conductivity in the studied system seem to have quite complex origin. A further investigation is required to determine which factor among those mentioned above plays the dominant role in altering the course of phase transition and its effect on the electrical conductivity.

To conclude, the samples prepared from powders obtained by sol-gel method as well as from those supplied by Alfa Aesar and heat-treated at  $800^\circ\text{C}$  exhibit phase transition from cubic to orthorhombic structure upon cooling below room temperature. In the course of phase transformation, the changes of the 400 X-ray reflection full width at half maximum correlate well with the changes in electrical parameters. The observed resistivity increase during phase transition depends on the procedure of spinel preparation. The phase transition is not complete even at  $-25^\circ\text{C}$  in the sample prepared from powder supplied by Sigma-Aldrich and no stepwise change of resistivity is observed for this sample. Additional impurity phases have been found and characterized in commercial samples, whereas the samples prepared by sol-gel method are single-phase after heat-treatment at  $800^\circ\text{C}$ . It can be deduced that presence of the impurity phases, especially  $\text{Li}_2\text{MnO}_3$  detected in powder supplied by Sigma-Aldrich, suppresses the phase transition of the lithium manganese spinel from cubic to orthorhombic

bic symmetry. The heat treatment of the commercial samples reduces the amount of impurity phases and amplifies the effect of phase transition upon conductivity. Although the present results do not provide any direct information on the performance of the studied lithium manganese oxide spinels as cathode materials in lithium-ion batteries, they imply caution when using lithium manganese oxide spinel from commercial suppliers in development of lithium-ion batteries, since the presence of impurity phases may cause deviation from stoichiometry and affect electrical properties of the spinel phase, leading to unexpected performance of the cathode.

*Acknowledgements.* This work has been supported by the Polish Committee for Scientific Research under grant KBN 3 T08A 006 26. The authors thank all of participants of the grant. Also V.N.Baumer thanks the International Centre for Diffraction Data for financial support (Grant #03-02).

## References

1. J.Pielaszek, J.R.Dygas, F.Krok et al., *Solid State Phenomena*, **130**, 63 (2007).
2. R.Dziembaj, M.Molenda, D.Majda et al., *Solid State Ionics*, **157**, 81 (2003).
3. D.Lisovytskiy, Z.Kaszur, N.V.Baumer et al., *Mol. Physics Repts.*, **35**, 26 (2002).
4. P.Endres, B.Fuchs, S.Kemmler-Sack et al., *Solid State Ionics*, **89**, 221 (1996).
5. Y.Gao, J.R.Dahn, *J. Electrochem. Soc.*, **143**, 1783 (1996).
6. V.Massarotti, D.Capsoni, M.Bini et al., *J. Solid State Chem.*, **128**, 80 (1997).
7. A.Yamada, *J. Solid State Chem.*, **122**, 160 (1996).
8. Y.Shimakawa, T.Numata, J.Tabuchi, *J. Solid State Chem.*, **131**, (1997)
9. J.Sugiyama, T.Atsumi, A.Koiwai et al., *J. Phys. Condens. Matter.*, **9**, 1729 (1997).
10. R.Kanno, M.Yonemura, T.Kohigashi et al., *J. Power Sources*, **97/98**, 423 (2001).
11. M.Tachibana, T.Tojo, H.Kawaji et al., *Phys. Rev. B*, **68**, 094421 (2003).

## Вивчення методами рентгенівської дифракції та імпедансної спектроскопії фазових переходів у нанокристалічних Li-Mn шпінелях

*Д.В.Лісовицький, В.М.Баумер*

Досліджено фазові переходи в нанокристалічних Li-Mn шпінелях, синтезованих методом золь-гель у лабораторних умовах, та у комерційних порошках  $\text{LiMn}_2\text{O}_4$ . Окрім стандартних вимірювань методами імпедансної спектроскопії та рентгенівським при геометрії Бреґга-Брентано, проведено одночасні вимірювання методами імпедансної спектроскопії та рентгенівським при нефокусуєчій геометрії у температурному діапазоні від  $-25^\circ\text{C}$  до  $+100^\circ\text{C}$ . З використанням рїтвельдївського аналізу кількісно оцінено фазовий склад зразків.